Segmentation of Gated Tl-SPECT Images for Automatic Computation of Myocardial Volume and Ejection Fraction

P Brigger, SL Bacharach, G Srinivasan, KA Nour, V Dilsizian, A Aldroubi, M Unser

National Institutes of Health, Bethesda, USA

Abstract

We present an algorithm for automatic assessment of left ventricular ejection fraction (EF) and absolute volume from gated Thallium-SPECT myocardial perfusion images. The system consists of two independent blocs for segmentation and computation of function. We introduce a novel formulation for computation of EF based on the epi-cardial contour. The algorithm was validated against manual border tracing from two physicians on different modalities, and gave consistent linear agreement: PET manual vs. automatic - avg. r = 0.91, Tl-SPECT manual vs. auto - r = 0.79. The new epicardial method was compared to the endocardial method, showing the former's improved performance at high noise. Finally, preliminary comparison were made of EFs computed for PET, ^{99m}Tc-SPECT and ^{201}Tl-SPECT to those obtained from planar gated blood pool imaging (GBP) yielding good results. The proposed scheme is specifically designed for ^{201}Tl-SPECT, but may be used on other image modalities as well. It permits EF computation on relatively noisy images without the need for additional image acquisitions.

1 Introduction

In the US, over 2 million ^{201}Tl-SPECT studies are performed each year, primarily to assess myocardial perfusion and viability. However, gating the SPECT images might permit one to compute several other clinically relevant parameters, such as ejection fraction (EF), myocardial mass, and wall thickening. This ability to quantify simultaneously both perfusion and functional information from a single study could result in a reduction in cost, time and radiation dose.

For PET and ^{99m}Tc-SPECT, several methods have been proposed for quantitative assessment of regional wall thickening [1, 2, 3, 4] and for automatic computation of EF [5, 6, 7, 8]. The benefits of automation lie in improved objectivity and consistency of the measured functional data. For successful automatic computation of EF, it has always been necessary to incorporate some physiological constraints. These may include minimal cavity size, smooth myocardial boundaries, or smooth temporal variation.

We propose here an image processing scheme specifically designed for noisier images, such as ^{201}Tl-SPECT. The key elements are a robust segmentation scheme that relies on a minimal number of threshold values, and a novel formulation of EF that is based on the epi-cardial contours, and which incorporates physiologic constraints. We first describe the segmentation bloc and the functionality bloc for EF computation, then the methods used to validate the technique, and finally the results of this validation.

2 Image processing system

The system is composed of a segmentation bloc and a functionality bloc, depicted in Fig. 1.

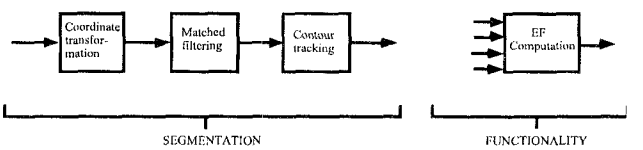

Figure 1: Image processing system

Segmentation: The segmentation bloc relies on three distinct processing steps. First, the image is transformed into an elliptical coordinate system. The change of coordinate system arranges the data in a form more suitable for segmentation, and permits measurement of true count profiles of the myocardium (i.e. profiles perpendicular to the heart wall). The second step in the segmentation process is matched filtering to enhance the endo- and epi-cardial boundaries. The change of coordinate system flattens the myocardium horizontally, so the filtering is performed selectively in the vertical direction. We have employed the simplest possible filters, which are two tap derivative

0276-6547/97 $10.00 © 1997 IEEE

convolutions. More complicated filters, derived from experimentally determined transition characteristics of the boundaries, may also be used. However, the exact shape of the convolution operator has little effect on the segmentation. The last step in the process is tracking of the desired contours. It is implemented by dynamic programming, which offers an efficient and robust way of solving the optimization problem. A more detailed description of the algorithm can be found in [9].

Functionality: The functionality bloc receives as input the absolute values of the volume of the endo- and epi-cardium for each time point t. Ejection fraction can then be computed as

$$EF = \frac{V_{endo}(t_D) - V_{endo}(t_S)}{V_{endo}(t_D)} \qquad (1)$$

where $V_{endo}(t_D) = \max_t[V_{endo}(t)]$ and $V_{endo}(t_S) = \min_t[V_{endo}(t)]$ are the end-diastolic and systolic volumes.

In the literature, (1) has been used exclusively to compute EF. However, it is not optimal for two reasons. 1) Equation (1) is extremely sensitive to noise because the result is based on only two values out of the N_t gating instances (the maximum and minimum value, respectively). 2) The endo-cardial boundary is more difficult to identify accurately than the epi-cardial boundary. This is because at low resolution, perfusion profiles of opposite walls may merge when the walls are close, (e.g. at systole), and also because of the possible presence of papillary muscle and blood background in the LV cavity.

We can reduce the effect of noisy data (particularly severe for ^{201}Tl-SPECT images) by considering all gating instances. It has been found in [10] that for EF computation, the volume curve can be described by two harmonics of a Fourier series. Hence, systole and diastole are found as the minimum and maximum of the smoothed data.

Addressing the second point above, we propose a novel method which uses the epi-cardial rather than the endo-cardial boundary to compute EF. The endo-cardial volume can be re-written as $V_{endo}(t) = V_{epi}(t) - m$, where m is the volume of the myocardium, and therefore EF is

$$EF = \frac{V_{epi}(t_D) - V_{epi}(t_S)}{V_{epi}(t_D) - m} \qquad (2)$$

Because myocardial mass, m, is conserved over the cycle, m can be obtained by averaging the difference between epi- and endo-cardial volume over the entire cycle. Therefore, the effect of outliers in the endo-cardial volume is reduced and the precision increased by a factor of $\sqrt{N_t}$. We show experimentally that this new approach produces the same results for noiseless images and better results for noisy images.

3 Methods

The algorithms were tested on images obtained from three different modalities. 1) Gated FDG-PET using 5mCi of ^{18}F-fluorodeoxyglucose, 17 patients, 2) Gated ^{99m}Tc-sestamibi SPECT, 9 patients, 3) Gated Thallium-201 SPECT, 32 subjects. Acquisition consisted of 8 or 10 gating instances. Four long axis slices (created by slicing the short axis set at 0°, 45°, 90°, and 135°) were created, resulting in a total of 32 or 40 images. For the validation experiments, we constructed a simulated Tl-SPECT image sequence by adding real SPECT noise to the FDG-PET images to obtain similar image noise characteristics. We chose the level of noise to produce a worst case scenario. The simulated Tl-SPECT sequence will be called PET-SPECT and is shown in Fig. 2.

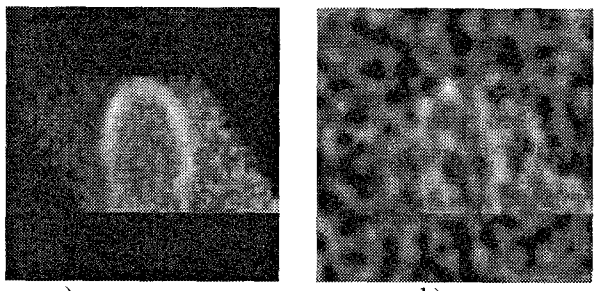

a) b)

Figure 2: a) Original PET image, b) PET-SPECT image with SPECT noise re-scaled and added to the PET image.

In a first experiment, we compared automatically obtained myocardial surface areas to surface areas obtained through manual border tracing by two physicians (p1 & p2), for PET, ^{201}Tl-SPECT and PET-SPECT images. We also compared the manually obtained borders by physician p1 with the manually obtained borders by physician p2 and verified that the automatically obtained values lay within the range of uncertainty of the manual tracers. The experiment was repeated on a second day, several weeks after the first. Hence, we were also able to study the intra-observer variability of the physicians. The experiment gives the relative precision of the automatic algorithm with respect to a manual border tracing.

We then tried to assess absolute accuracy by comparing manually and automatically obtained surface-areas from the PET-SPECT images to the surface-areas from the true underlying contours. We estimated the true values by averaging the values obtained by automatic border tracing, and by manual border tracing by p1 and p2.

Next, a third set of experiments was performed, intended to evaluate the effectiveness of computing EF based on the epi-cardial contour (Eq. (2) vs. a computation based on the endo-cardial contour (Eq. (1)).

For this purpose, we compared both methods of EF computation for the noise free PET images and the noisy PET-SPECT images. In the former case, a relatively good correlation between the two approaches should be observed, whereas in the latter case more fluctuations and a poorer correlation can be expected. It is also of interest to compare EF values based on the same formula obtained for the PET images vs. the EF values obtained for the PET-SPECT images. The better the correlation, the more stable is the EF computation.

Finally, we made a preliminary comparison of EFs obtained from rest gated blood pool imaging (GBP) with those obtained from the automatic algorithm (using Eq. (2)) for PET, Tc-SPECT and Tl-SPECT images.

4 Results

The results for assessment of the algorithm's accuracy can be summarized as follows. Manual contours were drawn by physicians p1 and p2 on two different days (separated by several weeks). The absolute epi-cardial surface areas of manual versus the new automatic algorithm were compared on each day. For PET data (drawn only on 1 day) the auto vs. manual slope averaged (over p1 and p2) <0.94> with an average intercept of <0.32>, and an <r>=0.91. For comparison, p1 versus p2 gave a slope of 0.78, intercept of 1.92 and r=0.85 - much poorer than the agreement with the automatic method and either p1 or p2. For Tl-SPECT the average (over p1 and p2) slope, intercept and r for auto vs. manual was <0.91>, <0.43> and <r>=<0.79>, again better than the inter-observer slope, intercept and r of 0.64, 1.87 and r=0.70. Finally, for the noisy PET-SPECT data the slope, intercept and r for auto vs. manual were <0.77>, <1.34> and <r>=<0.79>, compared to the inter-observer slope, intercept and r of 0.89, 0.56 and r=0.74.

Next we compared automatic and manual segmentation results on the PET-SPECT images to the true underlying contours as obtained from the noise free PET image. The automatically obtained contours show a better linear agreement than the manually obtained ones, (r = 0.88 for true vs. auto, compared to an average r of <0.75> for true versus manual), indicating better consistency. The difficulty that human observers have with the noisy PET-SPECT data is borne out by the poor intra-observer correlation, from day 1 to day 2, which for PET-SPECT was r=0.61 for p1 and r=0.79 for p2, and the poor inter-observer variability, yielding an average correlation of r=0.70.

One of the most valuable features of our system is its ability to handle very different types of images in an autonomous fashion. For all of the results presented in this article, the exact same parameters were used in all computations. This feature of robustness is very valuable for unsupervised processes and for situations in which input images may have differing resolution and signal-to-noise ratios.

Table I compares EF computed from endo-cardial boundaries (using Eq. (1)) versus EF computed from epi-cardial boundaries (using Eq. (2)). The first row compares the results based on the noise free original PET image and the second row considers the noisy PET-SPECT image.

A very good correlation (r=0.92) can be observed between the two types of measurements for the PET image. A calibration of the derivation operator for the matched filters could be applied to obtain unity slope. Hence, for less noisy images images, both (1) and (2) give essentially the same result. For the noisy PET-SPECT images (row two), the linear agreement is less good, and one needs to determine which formulation of EF is more accurate. The answer is given in rows three and four of Table I. Here, EFs obtained from the noiseless PET images and obtained from the noisy PET-SPECT images are compared using the same formula. Ideally, a unity correlation coefficient should be obtained. Clearly, computation of EF based on the epi-cardial contour (2) is more accurate for noisy images. For noiseless images, either formula (1) or (2) may be used.

Table I

Comparison of the formulas for EF based on the endo-cardial contours ($EF_{ENDO} = \frac{V_{endo}(t_D) - V_{endo}(t_S)}{V_{endo}(t_D)}$) and on the epi-cardial contours ($EF_{EPI} = \frac{V_{epi}(t_D) - V_{epi}(t_S)}{V_{epi}(t_D) - m}$). Compared are EFs for the noise free PET image and for the noisy PET-SPECT image.

	EF correlation
PET:	
EF_{ENDO} vs. EF_{EPI}	$y=7.2+1.5x;\ r=0.92$
PET-SPECT:	
EF_{ENDO} vs. EF_{EPI}	$y=5.9+1.46x;\ r=0.72$
EF_{ENDO}:	
PET vs. PET-SPECT	$y=13.3+0.54x;\ r=0.75$
EF_{EPI}:	
PET vs. PET-SPECT	$y=8.3+0.80x;\ r=0.86$

Finally, we performed preliminary comparisons between automatically computed EF measurements on gated PET, Tc-SPECT and Tl-SPECT images and EFs obtained from gated planar blood pool imaging. All the sets show a good linear agreement (PET: $y = 8.7 + 1.07x,\ r = 0.84$, Tc-SPECT: $y = 5.0 + 0.80x,\ r = 0.90$, Tl-SPECT $y = 23.5 + 0.82x,\ r = 0.77$, RMS error = 10.0). All of the segmented as well as the original image sequences can be dynamically viewed over the World Wide Web (http://picasso.ncrr.nih.gov/brigger/SPECT). It shows

how the algorithm interpolates over perfusion defects and how it handles images of low signal-to-noise ratio.

5 Discussion and Conclusions

We have introduced an algorithm for automatic EF computation and have presented extensive validation studies. We have decomposed the algorithm into two parts. The segmentation part is general, makes a minimal number of physiological assumption and requires few input parameters. The functionality part computes EF and incorporates physiological constraints.

Our experiences indicate that the algorithm produces EF values well within the uncertainty of the physicians. The automatic algorithm seems to provide a better representation of the true contour than does the manual analysis. This may be due in part to the integration of the temporal information, which can not be done manually.

A key results of this work is the computation of EF based on the epi-cardial contour. Our experiments indicate that there is a very high linear agreement with respect to the conventional method when the signal to noise ratio is high. Hence, up to a calibration factor, either method may be used for EF computation when the image quality is good. We have shown, however, that a computation based on the epi-cardial contour is advantageous and more reliable whenever the image signal to noise ratio is low, as in the case of Tl-SPECT images.

Finally, we performed a preliminary comparison between automatically computed EFs and EFs obtained from GBP images. The linear agreement for PET images is rather low, given the good image quality and our certainty about the automatically found boundaries. The values for GBP and PET images were separated by several months for some of the individuals and, although no treatment was conducted during that period, this could account for some of the discrepancy. The correlations for the ^{99m}Tc-SPECT images are based on a relatively small amount of data, but are consistent with those of [6, 8]. Finally, the correlation value for the ^{201}Tl-SPECT images is acceptable and encouraging bearing in mind the low signal-to-noise ratio of those images. As the correlation value reflects uncertainties of both the automatically obtained results and the values obtained from GBP, we can expect a better correlation with respect to the true data.

References

[1] K. Yamashita, N. Tamaki, Y. Yonekura, H. Ohtani, Y. Magata, R. Nohara, H. Kambara, C. Kawai, T. Ban and J. Konsihi, "Regional wall thickening of left ventricle evaluated by gated positron emission tomography in relation to myocardial perfusion and glucose metabolism", J Nucl Med, vol. 32, pp. 679-685, 1991.

[2] C.D. Cooke, E.V. Garcia, S.J. Cullom, T.L. Faber and R.I. Pettigrew, "Determining the accuracy of calculating systolic wall thickening using a fast fourier transform approximation: a simulation study based on canine and patient data", J. Nucl Med, vol. 35, pp. 1185-1192, 1994.

[3] C. Marcassa, P. Marzullo, O. Parodi, G. Sambuceti and A. L'Abbate, "A new method for noninvasive quantitation of segmental myocardial wall thickening using technetium-99m 2-methoxy-isobutyl-isonitrile scintigraphy - Results in normal subjects", J Nucl Med, vol. 31, pp. 173-177, 1990.

[4] G. Porenta et al., "Parameter Estimation of cardiac geometry by ECG-Gated PET imaging: validation using magnetic resonance imaging and echocardiography", Journ. of Nuclear Medicine, vol. 36, pp. 1123-1129, 1995.

[5] E.L. Dove, K. Philip, N.L. Gotteiner, M.J. Vonesh, J.A.R.J.E. Reed, W. Stanford, D.D. PcPherson and K.B. Chandran, "A method for automatic edge detection and volume computation of th eleft ventricle form ultrafast computed tomographic images", Investigative Radiology, vol. 29, no. 11, pp. 945-954, 1994.

[6] G. Germano, H. Kiat, P. Kavanagh, M. Moriel, M. Mazzanti, H. Su, K.V. Train and D. Berman, "Automatic quantification of ejection fraction from gated myocardial perfusion SPECT", *The Journal of Nuclear Medicine*, vol. 36, no. 11, pp. 2138-2147, November, 1995.

[7] G. Germano, J. Erel, H. Kiat, P. Kavanagh and D. Berman, "Quantitative LVEF and qualitative regional function from gated Thallium-201 perfusion SPECT", J Nucl Med, vol. 38, pp. 749-754, 1997.

[8] K. Nichols, E.G.D. Puey and A. Rozanski, "Automation of gated tomographic left ventricular ejection fraction", Journal of Nuclear Cardiology, vol. 3, no. 6, pp. 475-482, November/December, 1996.

[9] P. Brigger, S.L. Bacharach, A. Aldroubi and M. Unser, "Segmentation of gated SPECT images for automatic computation of myocardial volume and ejection fraction", in Int. Conf. on Image Proc. ICIP'97, Santa Barbara, CA, October 26-29, 1997. In press.

[10] S.L. Bacharach, M.V. Green, D. Vitale, G. White, M.A. Douglas, R.O. Bonow and S.M. Larson, "Optimum Fourier Filtering of Cardiac Data: A Minimum-Error Method: Concise Communication", Journal of Nuclear Medicine, vol. 24, no. 12, pp. 1176-1184, December, 1983.

Author's address: Patrick Brigger
BEIP/NCRR
13 South DR MSC 5766
NIH
Bethesda, MD 20982, USA
Tel.: (301) 435 1951
E-mail: brigger@helix.nih.gov